Catal Lett (2012) 142:657–663
DOI 10.1007/s10562-012-0823-3

# Low Temperature CO Oxidation on Ruthenium Oxide Thin Films at Near-Atmospheric Pressures

**Y. Martynova · B. Yang · X. Yu · J. A. Boscoboinik · S. Shaikhutdinov · H.-J. Freund**

Received: 8 February 2012 / Accepted: 7 April 2012 / Published online: 24 April 2012


**Abstract** Ruthenium model catalysts in the form of thin ruthenium oxide films grown on Ru(0001) were studied in the CO oxidation reaction at near-atmospheric pressures. The surfaces were prepared under vacuum conditions prior to the reactivity measurements carried out in a circulating flow reactor using gas chromatography. The films possessing oxygen in amounts equivalent to 1–4 monolayers (MLE) on Ru(0001) as determined by electron spectroscopy, exposed both the oxidic ($RuO_2$(110)-like) and O/Ru(0001) surfaces. In addition, one-dimensional oxide structures were observed by scanning tunneling microscopy, which are tentatively assigned to the intermediate state for a crystalline ruthenium oxide thin film that covered the entire surface at higher oxygen coverages. At low temperatures studied (400–470 K), the reaction sets in only in the presence of oxidic structures, i.e. when the oxygen coverage, on average, exceeds 1 MLE. The reaction rate slightly increases with increasing the nominal film thickness up to 7 MLE, reflecting primarily the lateral growth of oxide phases. The disordered oxide films showed even higher reactivity. The results suggest that surface ordering and oxide film thickness are not critical for the superior catalytic activity of ruthenium oxides in this reaction.

**Keywords** CO oxidation · Thin oxide films · Ruthenium oxide

Y. Martynova · B. Yang · X. Yu · J. A. Boscoboinik · S. Shaikhutdinov (✉) · H.-J. Freund
Abteilung Chemische Physik, Fritz-Haber-Institut der Max-Planck-Gesellschaft, Faradayweg 4-6, 14195 Berlin, Germany
e-mail: shaikhutdinov@fhi-berlin.mpg.de

## 1 Introduction

Well-ordered, thin oxide films have drawn some attention in recent years as suitable oxide supports for modeling highly dispersed metal catalysts at the atomic scale. It has been noticed, however, that the film thickness often influences the atomic structure and even the oxidation state of supported metal species due to the presence of a metal substrate underneath the film, which must be included in the proper description of such systems [1]. Not surprisingly, the ultra-thin oxide films exhibit physical and chemical properties different from the "thick" films which behave essentially as the bulk-like oxides [2, 3]. Indeed, our recent studies of iron oxide films grown on Pt(111) [4, 5] demonstrated that the film thickness may play an important role in oxidation reactions such as CO oxidation. At relatively low temperatures ($\sim$450 K), an ultra-thin FeO(111) film was found to be much more active than nm-thick $Fe_3O_4$(111) films and a Pt(111) support under the same conditions [4]. It has turned out that a bilayer FeO film, which is inert at low oxygen pressures, transforms into a trilayer, O–Fe–O film at higher oxygen pressures and catalyzes CO oxidation through a Mars-van Krevelen like mechanism [5–7]. In addition to the FeO(111)/Pt(111) system, the promotional effect of ultrathin oxide films in CO oxidation has been predicted also for the MgO(001) films on Ag(100), albeit through another reaction mechanism, both systems showing a much lower activation barrier than Pt(111) [8]. In both cases, the reaction is accompanied by a charge transfer that involves substantial surface reconstruction.

It is tempting to transfer these ideas also to "native" oxide films, which could, in principle, be even formed on noble metal surfaces, provided the high chemical potential of oxygen. In this respect, perhaps the most explored,

yet controversial example concerns Ru catalysts, which recently attracted much attention of the catalytic and surface science communities. The original ideas of Peden and Goodman [9–11] suggesting a dense (1 × 1) phase of chemisorbed oxygen on Ru(0001) as the active phase for CO oxidation have been revisited by Over and co-workers [12, 13] who suggested that, under technologically relevant conditions, the Ru catalyst is represented by the $RuO_2$(110) surface. The following-up studies of several research groups suggested that the active phase is a thin ruthenium oxide film, sometimes referred to as "surface oxide" [14–16].

This "ruthenium puzzle" triggered more elaborative studies on surface structures of other noble metal catalysts at elevated oxygen pressures. The formation of ultrathin oxide layers on Pt, Pd, and Rh, and their high reactivity in CO oxidation have recently been reported [17–22]. Interestingly, for the Rh surfaces, the highly active trilayer, O-Rh-O structures were observed [21, 22], pointing to a close similarity to the above-mentioned behavior of the ultrathin iron oxide films on Pt(111).

To the best of our knowledge, systematic studies of the reactivity of "native" oxide films as a function of the film thickness have not been performed, although in their recent paper Goodman and co-workers [23] mentioned similarities in the catalytic behavior of the ruthenium oxide films prepared at different oxidation temperatures. In this work, we have examined thin ruthenium oxide films on Ru(0001) in the CO oxidation reaction at near-atmospheric pressures and low temperatures (400–470 K). In particular, our study is focused on finding the relation between the reactivity of oxide films and the film thickness.

## 2 Methods and Materials

The experiments were carried out in the ultrahigh vacuum (UHV) chamber equipped with LEED, AES (Auger electron spectroscopy), and quadrupole mass-spectrometer for temperature programmed desorption (TPD) experiments. For reactivity measurements the double-side polished Ru(0001) crystal, mounted to the thin Ta wires for resistive heating, was transferred into the gold-plated high-pressure cell (~30 cc) connected to a gas chromatograph [4]. After introducing gas mixture at the room temperature and reaching the steady state flow, the sample was heated to the reaction temperature at the rate 1 K/s.

The O(2 × 1)-Ru(0001) surface was prepared by exposure to $2 \times 10^{-7}$ mbar $O_2$ at 420–450 K for 10 min [24]. The 3O(2 × 2) structure [25] was prepared by oxidation in $1 \times 10^{-6}$ mbar $O_2$ at 1220 K for 5 min and cooling in the same oxygen pressure down to 300 K. The O(1 × 1)-Ru(0001) surface was formed upon exposure to 20 mbar of $O_2$ at 450 K for 10 min. Thin oxide films on Ru(0001) were prepared by oxidation in $10^{-4}$ mbar of $O_2$ at 600–700 K. The film thickness was varied by the oxidation time and temperature. The surface composition was determined by AES using O(2 × 1)- and 3O(2 × 2)-Ru(0001) structures as the references. The nominal film thickness is presented in the text in oxygen monolayer equivalents (MLE) such that 1 MLE corresponds to the amount of the surface oxygen atoms in the (1 × 1) O-Ru(0001) structure.

Further structural characterization of the prepared surfaces was performed in another UHV chamber equipped with LEED, scanning tunneling microscopy (STM) and x-ray photoelectron spectroscopy (XPS).

## 3 Results and Discussion

A variety of Ru model catalysts were first prepared and characterized under UHV conditions prior to the reactivity measurements performed at near-atmospheric pressures. At low oxygen coverage (below 1 MLE, see Methods and Materials), the surfaces exposed ordered structures, such as O(2 × 1)- and 3O(2 × 2)-Ru(0001), with the oxygen atoms only chemisorbed on the surface (henceforth referred to as oxygen adlayer structures). Upon deeper oxidation (oxygen coverage >1 MLE) the surfaces showed LEED patterns characteristic for the $RuO_2$(110) overlayer on Ru(0001) [26] (referred to as oxide films). The CO oxidation reaction was carried out in a circulating mixture of CO and $O_2$ in the mbar-pressure range balanced by He to 1 bar at a crystal temperature of 400–450 K. AES and LEED characterization of the oxide films after the reaction revealed practically the same surface composition and ordering, suggesting no substantial structural transformations under the reaction conditions. In contrast, metallic Ru(0001) and oxygen adlayer structures are all transformed into the O(1 × 1)-Ru(0001) phase. This is in variance to the high temperature reaction conditions (>550 K) where the oxide formation on Ru(0001) is observed *during* the reaction [13–15].

The kinetic curves of $CO_2$ production under net oxidizing conditions (10 mbar CO; 50 mbar $O_2$) at 450 K are shown in Fig. 1. For oxide films, the $CO_2$ production first grows linearly in time, then slows down and stops as CO is totally consumed. It is clear that thin oxide films are much more active than the O/Ru(0001) surfaces. In order to quantitatively compare the intrinsic activity of these model catalysts, one has to measure the reaction rate at zero conversion over non-deactivated surfaces. This is difficult to do for the very active oxide films studied here, showing almost 100 % conversions within 15 min of the reaction. However, the nearly constant reaction rate even at high CO

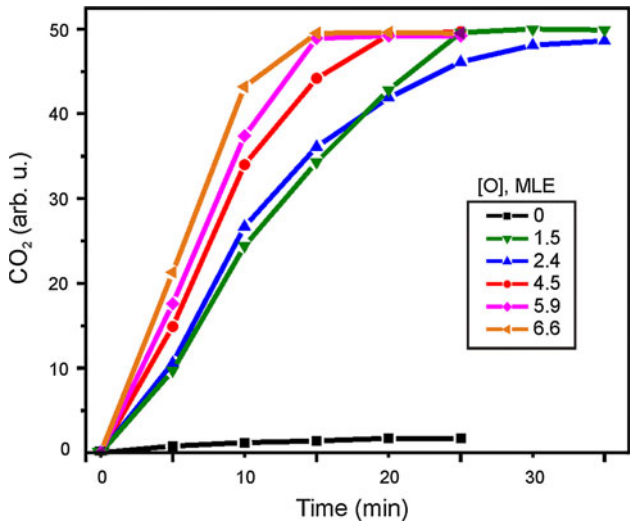


**Fig. 1** Reaction kinetics for CO oxidation on clean Ru(0001) crystal and thin oxide films grown on Ru(0001), possessing the indicated amounts of oxygen (in MLE) prior to the reaction. The $CO_2$ production was measured in the circulating mixture of 10 mbar CO and 50 mbar $O_2$ (He balance) at crystal temperature of 450 K

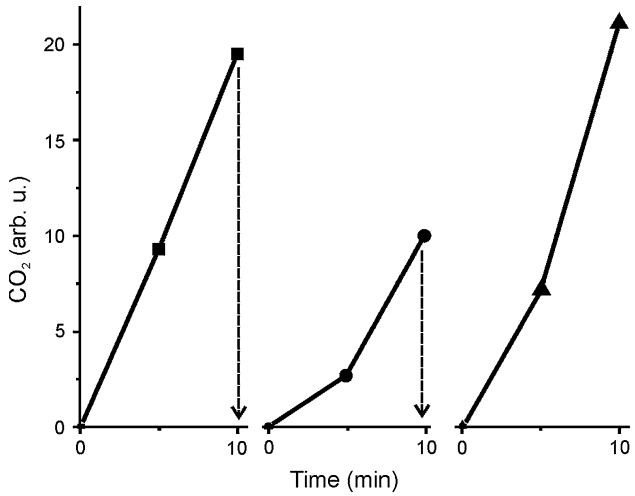


**Fig. 2** Sequential CO oxidation runs over a 5 MLE film at 450 K. After 10 min of the reaction in the 10 mbar CO and 50 mbar $O_2$ (He balance) mixture, the reactor was pumped off, and the sample cooled down to ~300 K. Then, the reactor was refilled with a fresh CO + $O_2$ mixture, and the reactivity was measured at 450 K. After the second run the sample was flashed to 600 K in UHV prior to refilling the reactor

conversions implies no poisoning by $CO_2$ that is accumulated in the circulating mixture. To further prove this conclusion, we have performed the following experiment as shown in Fig. 2.

After 10 min of the reaction at 450 K the reactor was pumped out while cooling the sample to the room temperature. Then, the reactor was re-filled with the fresh CO + $O_2$ mixture, heated up to the reaction temperature, and the reactivity was measured again. In the beginning, the $CO_2$ production rate slightly diminished, most likely because of carbonaceous deposits formed during sample cooling and gas pumping out, but it recovered to the original value upon the carbon burnout in the excess of oxygen. Indeed, when the same procedure was repeated except the sample has been flashed to 600 K in UHV prior to refilling the reactor, the reaction proceeds with the same rate from the onset. Therefore, the results suggest that the reactivity of oxide films at 450 K does not suffer from the presence of $CO_2$ in the reaction mixture, at least under net oxidizing conditions. This finding allowed us to compare the reactivity of oxide films by measuring the $CO_2$ production rate within the first 10 min of the reaction. The turnover frequencies (TOF) were derived as the number of produced $CO_2$ molecules per second per active sites, whose density was set to $10^{15}$ at/cm$^2$, for simplicity, as the number of active sites on O(1 × 1)-Ru(0001) and oxide structures may be different, in particular for the non-uniform films.

When re-plotted in terms of the reaction rates, Fig. 3 clearly shows a steep increase in the reactivity upon oxygen incorporation into the Ru surface (i.e. oxygen coverage exceeds 1 MLE). Basically, the CO oxidation reaction sets in only in the presence of oxide phase. Increasing of the nominal film thickness further enhances the reactivity, but to the lower extent. These results suggest that the presence of a very thin oxide layer is, in principle, sufficient to show superior catalytic activity, whereas O-precovered Ru(0001) is inactive under the conditions studied.

To gain further information about the atomic structure of the films, we have performed STM studies in another UHV chamber, where the oxygen coverage was determined by XPS. The surfaces were prepared in the same way as studied above. Relatively thick films (>4 MLE) exhibited

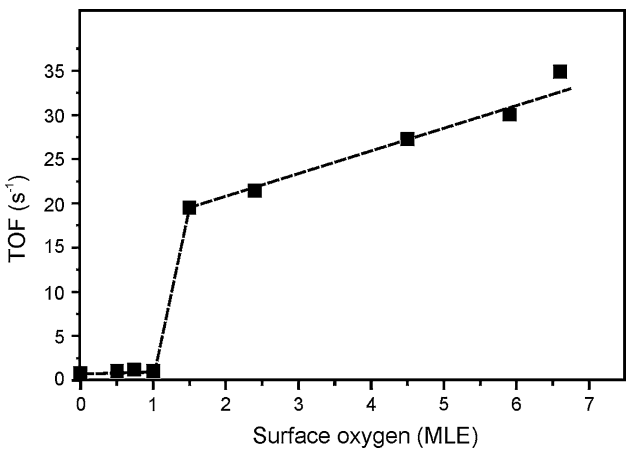


**Fig. 3** $CO_2$ formation rate (TOF), measured within the first 10 min of the reaction (see Fig. 1), as a function of surface oxygen coverage measured prior to the reaction. The reaction was performed in the circulating mixture of 10 mbar CO and 50 mbar $O_2$ (He balance) at 450 K

sharp LEED patterns of $RuO_2(110)$/Ru(0001) and showed STM images very similar to the previously reported by Over et al. [12] and Rössler et al. [27], with rectangular-shaped terraces dominating the large scale morphology (Fig. 4a). High resolution STM images (inset in Fig. 4a) revealed the atomic structure characteristic for the $RuO_2(110)$ surface, where the protruding lines with a $\sim$6.5 Å spacing were assigned to the bridging oxygen atoms in the bulk rutile structure of $RuO_2$ [26]. At these high oxygen coverages, an oxide film uniformly covered the entire crystal surface as judged by STM and CO TPD experiments (not shown).

In contrast, the ultra-thin films (i.e., 1–2 MLE), showing faint diffraction spots of $RuO_2(110)$, exhibited very heterogeneous surface, with patches of $RuO_2(110)$ coexisting with the $(1 \times 1)$O-Ru(0001) surface. In addition, new row-like structures were observed by STM as shown on Fig. 4b. The protruding rows were primarily running along the $[10\bar{1}0]$ direction, i.e. the same as for $RuO_2(110)$ overlayer. However, the rows exhibited a $\sim$4.6 Å periodicity along the rows (see inset in Fig. 4b), which is considerably larger than observed for the bridging oxygen rows on $RuO_2(110)$, i.e. 3.1 Å. Also the spacing between the rows (e.g. $\sim$9 Å, on average) is definitely larger than the distance between adjacent rows on $RuO_2(110)$ (=6.4 Å). For the isolated rows it was possible to see by STM that the "open" surface between the rows exhibits the honeycomb-like $3O(2 \times 2)$-Ru(0001) structure (inset in Fig. 4b). Tentatively, we have assigned these rows to the one-dimensional oxide structures as an intermediate state and/or precursor to the formation of $RuO_2(110)$ overlayer. Certainly, determination of its atomic structure needs further studies. Nonetheless, thermal desorption spectra of oxygen on the oxide films of various thicknesses did not reveal any new features beyond those observed on the "thick" $RuO_2(110)$ films. Upon exposure to 10 mbar $O_2$ at 450 K all the films studied showed $O_2$ desorption signal at $\sim$420 K, previously assigned to terminal oxygen [28], and the main peak centered at $\sim$1010 K resulted from the film decomposition. The intensity of both peaks basically scaled with increasing the nominal film thickness. Therefore, combined together the LEED, STM, and TPD results suggest the increase of the reaction rate above 1 MLE, shown in Fig. 3, due to the increasing the surface fraction covered by an oxide (not necessarily $RuO_2(110)$) phase.

The apparent activation energy and the reaction orders for CO and $O_2$ were only measured for the 5 MLE films, where $RuO_2(110)$ covered the entire surface. A freshly prepared film of the same composition was prepared for each experiment. In the reaction mixture of 10 mbar CO and 50 mbar $O_2$ the Arrhenius plot in the temperature range of 400–470 K yields the activation energy ca. 58 ($\pm$4) kJ/mol (Fig. 5). This value is considerably lower than 78 $\pm$ 10 kJ/mol reported for the 1.6 nm $RuO_2(110)$/Ru(0001) film and measured at the nearly stoichiometric $CO/O_2$ ratios (14 mbar CO + 5.5 mbar $O_2$) at 470–670 K [29].

The reaction orders were determined by measuring reactivity at different $CO/O_2$ ratios at 430 K. In one set of the experiments, the partial pressure of $O_2$ was set to 20 mbar, and the CO pressure was varied (Fig. 6a). In another set, the CO pressure was set to 10 mbar, and the oxygen pressure was varied (Fig. 6b). Again, for each experiment, a new film with the same surface composition was prepared. The results, shown in Fig. 6c, revealed the first order reaction for CO and practically zero order for $O_2$.

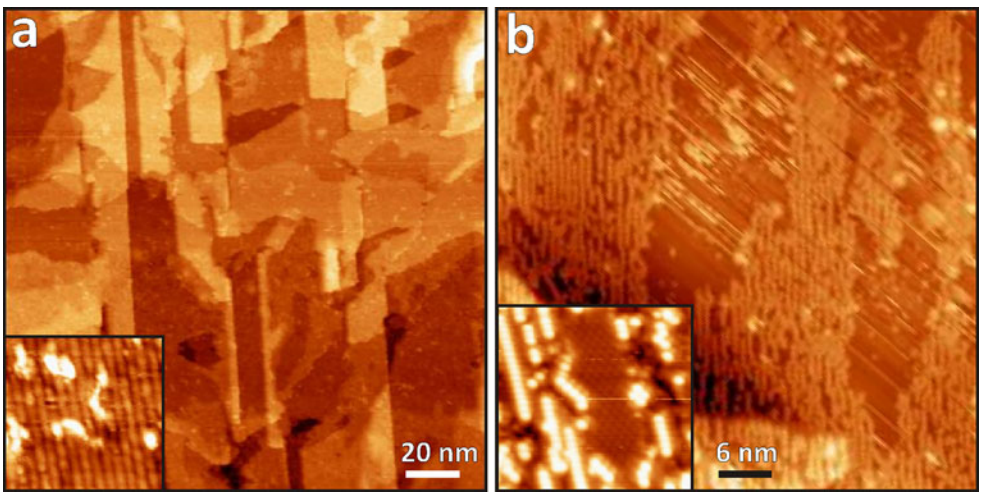


**Fig. 4** **a** Typical large-scale STM image of "thick" (>4 MLE) films. The *inset* shows a high-resolution image characteristic for the $RuO_2(110)$ surface, with a $\sim$6.5 Å spacing between the protruding rows. **b** STM image of row-like structures additionally observed on the ultra-thin films (1–2 MLE). (The streaks are caused by the tip instability along the scanning direction). The *inset* shows atomically resolved STM image of the rows as well as $3O(2 \times 2)$-Ru(0001) structure in between

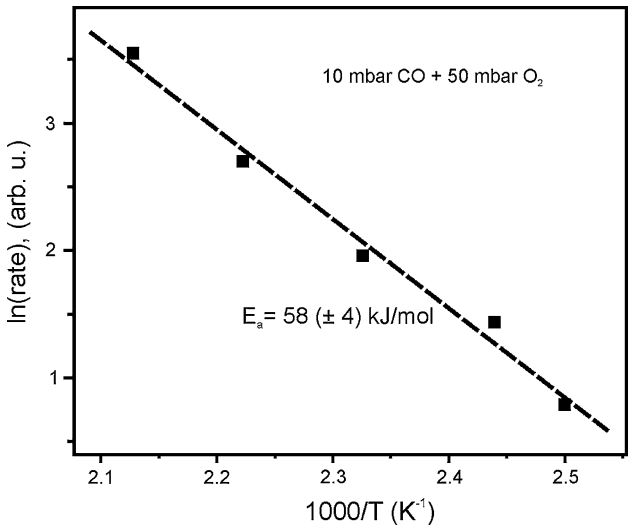


**Fig. 5** The Arrhenius plot for CO oxidation over 5 MLE oxide films on Ru(0001) in 10 mbar CO + 50 mbar $O_2$ (He balance)

(Note, that zero orders for both CO and $O_2$ on the $RuO_2$(110) films under net oxidizing conditions were reported by Over et al. [29], which were, however, determined only qualitatively by varying partial pressures of both gases simultaneously).

The reaction kinetics, presented in Figs. 6(a,b), clearly show the catalysts deactivation with time. Several mechanisms for the deactivation have been discussed in the literature: a surface reconstruction into a less active phase [30] and a carbonaceous (e.g., a carbonate) contamination mechanism [23, 27]. Which of these two is operative in our experiments is difficult to ascertain on the basis of solely AES and LEED characterizations of the post-reacted surfaces. Note only, that the results of Fig. 2 for the highly active films showed no $CO_2$ self-poisoning effect otherwise expected for the carbonate mechanism. It therefore appears that the deactivation is a relatively slow process, at least under net oxidizing conditions (see Fig. 1).

It is instructive now to compare our results with the recent work of Gao et al. [23], where the reactivity of pre-formed $RuO_2$(110) films was studied. Note, however, that the activity was determined from the pressure changes monitored with a baratron gauge using the entire UHV chamber (61.6 l) as the reactor. Also, the reactant mixture was renewed each time when the conversion exceeded 10 %. Nonetheless, these authors demonstrated that under net oxidizing conditions and relatively low temperatures (<450 K) $RuO_2$ displays higher activity than the (1 × 1)O-Ru(0001) phase, i.e. in full agreement with our results. It was stressed, however, that this high reactivity regime for $RuO_2$ is restricted: (1) to very oxidizing reaction conditions (2) to very low reaction temperatures, and (3) to short reaction times. Although these are, basically, the conditions used in the present work, our results indicate that the decisive parameter is the low reaction temperature, at which the (pre-formed) $RuO_2$(110) films are more active than metallic Ru(0001) regardless of the CO:$O_2$ ratio and reaction time. (Gao et al. [23] also found that even after 240 min of the reaction the oxide film was more active than (1 × 1)O-Ru(0001)). It seems the only discrepancy that remains between these two studies is the Gao et al's finding of a "negative" activation energy at $T < 475$ K in the mixture of 8 Torr CO and 40 Torr $O_2$ (see Figs. 7a and 8 in [23]), that has never been reported for any technical or model Ru catalysts. Meanwhile, our results show a regular behavior, with activation energy of ca 58 kJ/mol (see Fig. 5). In order to explain the rate decreasing with the temperature in the range 400–475 K, Gao et al. invoked the formation of a carbonate which deactivates the active sites at low temperatures, but dissociates upon approaching 500 K. However, this explanation implies that the carbonate overlayer was formed *before* the reactivity was measured. In contrast, our experiments, shown in Fig. 2, suggest that the presence of $CO_2$ (as a precursor for a carbonate) does not change the reaction rate, at least on the most active films. On the basis of the CO stretch signal

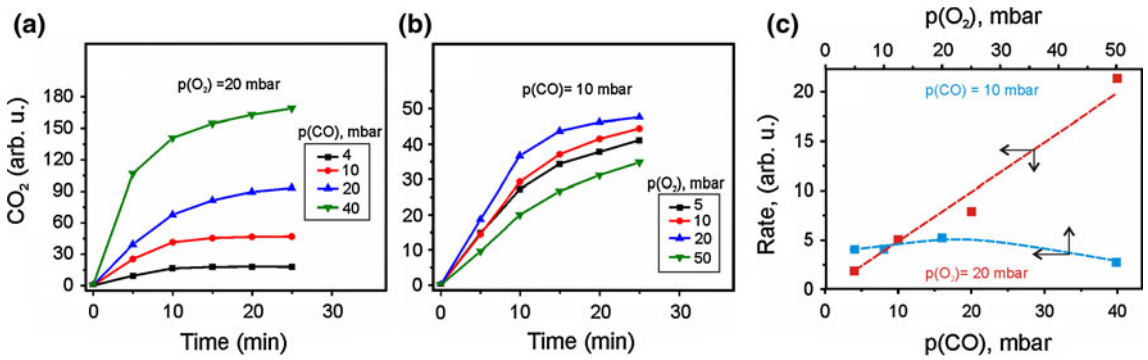


**Fig. 6** Pressure dependence of the CO oxidation reaction on 5 MLE films at 430 K. The CO pressure was varied at fixed $p(O_2) = 20$ mbar, while the $O_2$ pressure was varied at fixed $p(CO) = 10$ mbar (He balance). Each *curve* corresponds to a new film

intensity in the PM-IRAS spectra, Gao et al. concluded that in this "negative activation" regime the net CO coverage *increases* with temperature. However, it is well known that the relation between the IRAS intensity and the site population is not straightforward. Overall, we believe that the observation of the "negative" activation energy reported by Gao et al. remains puzzling and needs further studies.

Finally, in order to see the effect of surface ordering on the reaction, we have measured reactivity of the disordered films for comparison. For this, freshly prepared oxide films were subjected to mild $Ar^+$-sputtering (500 eV) followed by re-oxidation in $10^{-4}$ mbar $O_2$ at 450 K, i.e., much below the temperature used for the preparation of ordered films ($\sim$700 K). These treatments resulted in the disappearance of the diffraction spots of the $RuO_2$(110) phase, although no considerable changes in the surface stoichiometry were observed by AES. Nonetheless, for the two thicknesses studied (4.5 and 6.5 MLE), the disordered films exhibited higher reaction rate than the ordered films (Fig. 7). Therefore, the reactivity of oxide surface is not related to the surface ordering, thus suggesting that CO oxidation over the ruthenium oxide surfaces is, in fact, structure insensitive. Therefore, the rate enhancement, observed for the disordered films, could, in principle, be explained by the increased surface area of the roughened surfaces. These results agree well with the previous high pressure (0.1 mbar, $CO:O_2 = 1$) XPS studies showing no direct correlation between the high $CO_2$ production rate and the formation of the stoichiometric $RuO_2$ phase [15].

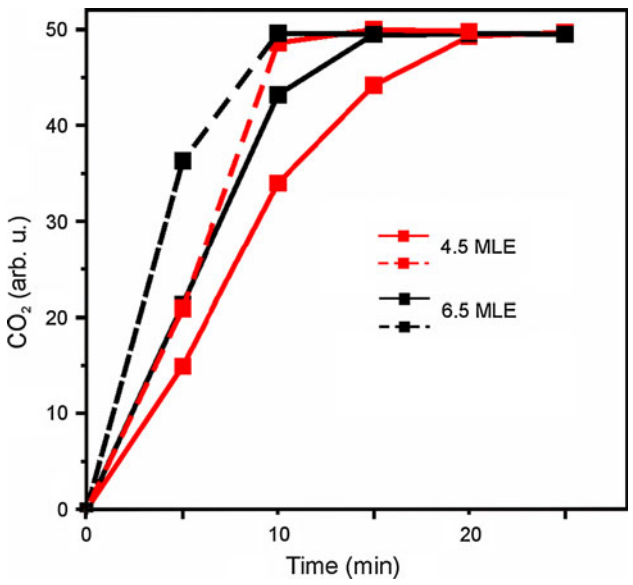


**Fig. 7** Effects of surface ordering on the reactivity of thin oxide films on Ru(0001) at 450 K. *Solid* and *dashed lines* show the results for ordered and disordered films, respectively, at two thicknesses as indicated. The disordered surfaces were prepared by 500 eV $Ar^+$ sputtering at 300 K and re-oxidation in $10^{-4}$ mbar $O_2$ at 450 K

## 4 Summary and Conclusions

Thin ruthenium oxide films grown on Ru(0001) and O-chemisorbed layers on Ru(0001) were studied in the CO oxidation reaction at near-atmospheric pressures at low temperatures (400–470 K). The surfaces were prepared under vacuum conditions prior to the reactivity measurements, which were performed using a gas chromatography. The surface composition, before and after reaction, was monitored by electron spectroscopy.

For the ultra-thin films (1–2 MLE), the surface exposed both the $RuO_2$(110) and O-adlayer structures. In addition, one-dimensional oxide structures were observed, which were tentatively assigned to the intermediate state for a crystalline oxide thin film that covers the entire crystal surface at higher oxygen coverage.

It is shown that the CO oxidation reaction sets in only in the presence of the oxide phase. The reaction rate slightly increases with increasing the nominal film thickness up to 7 MLE, reflecting primarily the lateral growth of oxide phases. The disordered oxide films showed even higher reactivity. The results suggest that surface ordering and oxide film thickness are not critical for the superior catalytic activity of ruthenium oxides in this reaction.

## References

1. Freund HJ, Pacchioni G (2008) Chem Soc Rev 37:2224
2. Netzer F, Allegretti F, Surnev S (2010) J Vac Sci Technol B 28:1
3. Giordano L, Pacchioni G (2011) Acc Chem Res 44:1244
4. Sun YN, Qin ZH, Lewandowski M, Carrasco E, Sterrer M, Shaikhutdinov S, Freund HJ (2009) J Catal 266:359
5. Sun YN, Giordano L, Goniakowski J, Lewandowski M, Qin ZH, Noguera C, Shaikhutdinov S, Pacchioni G, Freund HJ (2010) Angew Chem Int Ed 49:4418
6. Lei Y, Lewandowski M, Sun YN, Fujimori Y, Martynova Y, Groot IMN, Meyer R, Giordano L, Pacchioni G, Goniakowski J, Noguera C, Shaikhutdinov S, Freund HJ (2011) ChemCatChem 3:671
7. Lewandowski M, Groot IMN, Shaikhutdinov S, Freund HJ (2012) Catal Today 181:52
8. Hellman A, Klacar S, Grönbeck H (2009) J Am Chem Soc 131:16636
9. Peden CHF, Goodman DW (1986) J Phys Chem 90:1360
10. Peden CHF, Goodman DW (1991) Surf Sci 253:44
11. Goodman DW, Peden CHF, Chen MS (2007) Surf Sci 601:L124
12. Over H, Kim YD, Seitsonen AP, Wendt S, Lundgren E, Schmid M, Varga P, Morgante A, Ertl G (2000) Science 287:1474
13. Kim YD, Over H, Krabbes G, Ertl G (2001) Top Catal 14:95
14. Narkhede V, Aßmann J, Muhler M (2005) Z Phys Chem 219:979
15. Blume R, Hävecker M, Zafeiratos S, Teschner D, Kleimenov E, Knop-Gericke A, Schlögl R, Barinov A, Dudin P, Kiskinova M (2006) J Catal 239:354
16. Rosenthal D, Girgsdies F, Timpe O, Blume R, Weinberg G, Teschner D, Schögl R (2009) Z Phys Chem 223:183
17. Hendriksen BLM, Frenken JWM (2002) Phys Rev Lett 89:046101-1

18. Hendriksen BLM, Bobaru SC, Frenken JWM (2004) Surf Sci 552:229
19. Lundgren E, Kresse G, Klein C, Borg M, Andersen JN, De Santis M, Gauthier Y, Konvicka C, Schmid M, Varga P (2002) Phys Rev Lett 88:246103-1
20. Ackermann MD, Pedersen TM, Hendriksen BLM, Robach O, Bobaru SC, Popa I, Quirós C, Kim H, Hammer B, Ferrer S, Frenken JWM (2005) Phys Rev Lett 95:255505-1
21. Gustafson J, Mikkelsen A, Borg M, Lundgren E, Köhler L, Kresse G, Schmid M, Varga P, Yuhara J, Torrelles X, Quirós C, Andersen JN (2004) Phys Rev Lett 92:126102-1
22. Gustafson J, Westerström R, Mikkelsen A, Torreles X, Balmes O, Bovet N, Andersen JN, Baddeley CJ, Lundgren E (2008) Phys Rev B 78:045423-1
23. Gao F, Wang Y, Cai Y, Goodman DW (2009) Surf Sci 603:1126
24. Madey TE, Engelhardt H, Menzel D (1975) Surf Sci 48:304
25. Kostov KL, Gsell M, Jakob P, Moritz T, Widdra W, Menzel D (1997) Surf Sci Lett 394:L138
26. Kim YD, Seitsonen AP, Over H (2000) Surf Sci 465:1
27. Rössler M, Günther S, Wintterlin J (2007) J Phys Chem C 111:2242
28. Kim YD, Seitsonen AP, Wendt S, Wang J, Fan C, Jacobi K, Over H, Ertl G (2001) J Phys Chem B 105:3752
29. Over H, Balmes O, Lundgren E (2009) Catal Today 145:236
30. Aßmann J, Crihan D, Knapp M, Lundgren E et al (2005) Angew Chem Int Ed 44:917